Step bunching of vicinal 6*H*-SiC{0001} surfaces

Valery Borovikov* and Andrew Zangwill†
School of Physics, Georgia Institute of Technology, Atlanta, Georgia 30332, USA
(Received 10 March 2009; published 10 June 2009)

We use kinetic Monte Carlo simulations to understand growth-induced and etching-induced step bunching of 6*H*-SiC{0001} vicinal surfaces oriented toward $\langle 1\bar{1}00\rangle$ and $\langle 11\bar{2}0\rangle$. By taking account of the different rates of surface diffusion on three inequivalent terraces, we reproduce the experimentally observed tendency for single bilayer height steps to bunch into half unit-cell height steps. By taking account of the different mobilities of steps with different structures, we reproduce the experimentally observed tendency for adjacent pairs of half unit-cell height steps to bunch into full unit-cell height steps. A prediction of our simulations is that growth-induced and etching-induced step bunching lead to different surface terminations for the exposed terraces when full unit-cell height steps are present.

DOI: 10.1103/PhysRevB.79.245413 PACS number(s): 81.10.Aj, 81.15.Kk, 81.65.Cf

I. INTRODUCTION

Silicon carbide (SiC) is a very promising material for microelectronic applications because of its superior electronic properties, high thermal and chemical stabilities, high-power and high-frequency capabilities, and high tolerance to radiation damage.[1,2] SiC is also an attractive candidate as a substrate for the heteroepitaxial growth of other materials.[3,4] A particularly exciting example (which motivated the present study) is the growth of epitaxial graphene by thermal decomposition of the basal surfaces of single-crystal 4*H* and 6*H* SiCs.[5] Nevertheless, SiC will not reach its anticipated potential until a variety of problems are solved, not least being the need to controllably grow device-quality single-crystal material on a large scale.[1,2,6]

One approach to the growth problem is "step-controlled" epitaxy, where new layers grown onto surfaces vicinal to the hexagonal basal planes inherit the stacking order of the substrate through the step-flow mode of growth.[1] Unfortunately, step-flow growth on vicinal surfaces does not always proceed by the uniform motion of a train of evenly spaced steps. Instead, growth-induced step bunching often occurs, as it invariably does when vicinal surfaces are etched by exposure to hot hydrogen gas. Suggestions for the origin of SiC step bunching include impurity adsorption,[7,8] differences in surface energetics for different bilayers of α-SiC polytypes,[9–12] differences in intrinsic step velocities and step configurations,[9,10,13] and other differences in growth kinetics.[14,15] However, no systematic exploration of any particular mechanism and comparison of the results with all available data seems to have been performed until now.

This paper reports the results of kinetic Monte Carlo (KMC) simulations designed to identify the kinetic pathways that promote growth-induced and etching-induced step bunching of vicinal 6*H*-SiC surfaces. We focus on surfaces vicinal to (0001) (Si-terminated) and $(000\bar{1})$ (C-terminated) with steps running perpendicular to the $\langle 1\bar{1}00\rangle$ and $\langle 11\bar{2}0\rangle$ directions. These particular starting surfaces were chosen to make contact with experimental observations made using atomic force microscopy (AFM), low-energy electron diffraction analysis, high-resolution transmission electron microscopy (HRTEM), and scanning tunneling microscopy.[9,16–21] Our main conclusion is that the experimental results for the Si face are quite explicable using a lattice model that recognizes that there are three inequivalent terraces for surface diffusion and two inequivalent steps with different mobilities. The C-face data are similarly explicable (or at least rationalizable) if the terrace diffusion rates and step mobilities are less different on this face than on the Si face.

II. PREVIOUS WORK

A. Experimental observations

This section reviews the experimental observations of etching-induced and growth-induced bunching for surfaces vicinal to the basal planes of 6*H*-SiC. The designation 6*H* refers to the bulk unit cell indicated in Fig. 1 where six bilayers of silicon and carbons atoms are arranged in the particular stacking sequence shown. If it were exposed to vacuum, the top layer of silicon atoms would be a typical

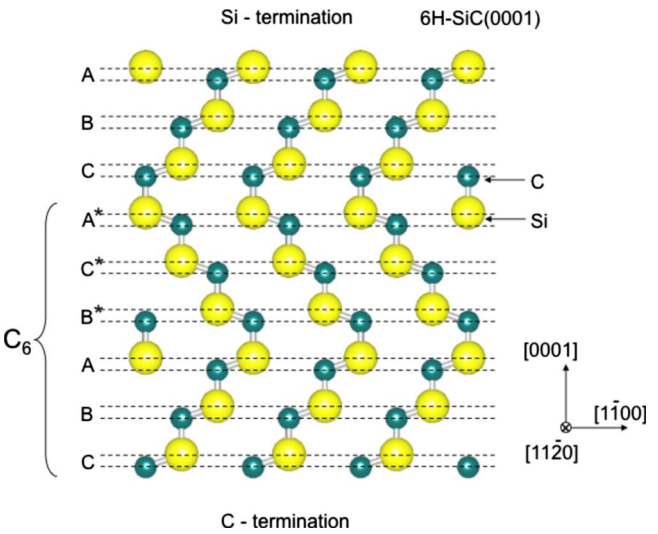

FIG. 1. (Color online) Arrangement of Si and C atoms in 6*H*-SiC crystal. A fragment of $(11\bar{2}0)$ atomic plain is shown schematically.

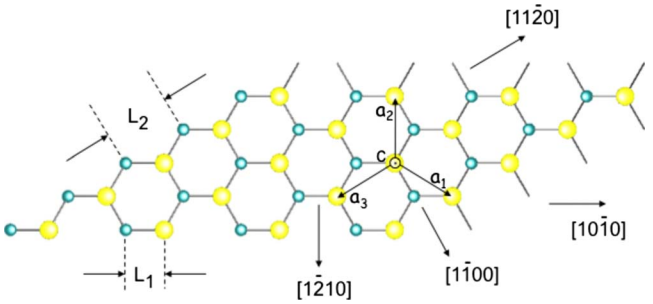

FIG. 2. (Color online) Top view of a single bilayer is shown schematically. L_1 and L_2 are the units of length in $\langle 1\bar{1}00\rangle$ and $\langle 11\bar{2}0\rangle$ directions, correspondingly.

(0001) Si-terminated surface. The bottom layer of carbon atoms similarly exposed would be a typical $(000\bar{1})$ C-terminated surface. Along the c axis of 6H-SiC crystal, the bilayers are arranged in two groups of three bilayers each. Each bilayer is exactly the same apart from rigid lateral shifts within one group of bilayers and rotation of the lattice by 60° around the c axis from one group of bilayers (A,B,C) to the other (A^*,C^*,B^*). The hexagonal arrangement of atoms shown in Fig. 2 is a (projected) view along [0001] of one of the bilayers from the $A^*C^*B^*$ group seen in edge view in Fig. 1.

There have been many experimental studies of growth[7–10,17,22–24] and etching[16,18–21] of 6H SiC surfaces cut slightly vicinal to its basal planes. The details vary (temperature, doping, and Si/C ratio during growth), but most papers focus on the Si-terminated face with miscuts oriented along the $\langle 11\bar{2}0\rangle$ direction. Only a few report results for the C-terminated surface or for vicinal miscuts oriented along the $\langle 1\bar{1}00\rangle$ direction. For our purposes the systematic H-etching experiments conducted by Feenstra and coworkers are particularly valuable.[20] Table I summarizes their AFM and HRTEM observations for nominally on-axis samples and samples with intentional miscuts of ~3° and 12°. The numbers $\frac{1}{2}$ and 1 in the table refer to observations of more or less ordered arrays of bunches where three Si-C bilayer steps have bunched into a single step with the height of $\frac{1}{2}$ unit cell and where two such bunches have further bunched into one unit-cell height steps. Etching of (0001) surfaces miscut 12° along $\langle 1\bar{1}00\rangle$ produces increased bunching into 4–5 unit-cell height steps which may more properly be regarded as "nanofacets."[18] For the same surface miscut 12° along $\langle 11\bar{2}0\rangle$, the authors find no average step orientation due to large-scale step meandering. From the corresponding image of the C face, we infer (hence the quotation marks in the table) similar, but less pronounced, step meandering. Quite generally, the data summarized Table I demonstrate that the tendency for etching-induced bunching is greater on the Si face than on the C face and greater for steps oriented perpendicular to $\langle 1\bar{1}00\rangle$ than for steps oriented perpendicular to $\langle 11\bar{2}0\rangle$.

TABLE I. Experimentally observed etching-induced step bunching of (0001) (Si-terminated) and $(000\bar{1})$ (C-terminated) surfaces of 6H-SiC for various miscut angles and orientations. Entries in quotation marks are inferred by the present authors. See text for discussion.

6H SiC(0001) Etching Results (Ref. 20)			
vicinal angle	<0.3°	~3°	12°
	Si terminated		
$[1\bar{1}00]$	1	1	4–5
$[11\bar{2}0]$	"1/2"	1/2	meander
	C terminated		
$[1\bar{1}00]$	1/2	"1"	1
$[11\bar{2}0]$	"1/2"	1	"meander"

There is no single data set for growth-induced step bunching comparable to the etching-induced results summarized in Table I. Nevertheless, a survey of the literature reveals trends very similar to the etching data. Thus, for surfaces miscut by 3.5° toward $\langle 11\bar{2}0\rangle$, Kimoto *et al.*[9] find that growth on Si-terminated surfaces produces $\frac{1}{2}$ unit-cell height bunches while growth on comparable C-terminated surfaces is twice as likely to remain completely unbunched (only SiC bilayer steps appear) as to bunch into $\frac{1}{2}$ unit-cell height steps. Similarly, data obtained for step-flow growth on vicinal Si-terminated surfaces oriented toward $\langle 1\bar{1}00\rangle$ exhibit six bilayer bunches (full unit cell), compared to only three bilayer bunches (half unit cell) observed for similar surfaces miscut along $\langle 11\bar{2}0\rangle$.[17] Therefore, as during etching, the tendency for growth-induced bunching is greater on the Si face than on the C face and greater for steps oriented perpendicular to $\langle 1\bar{1}00\rangle$ than for steps oriented perpendicular to $\langle 11\bar{2}0\rangle$. For both growth and etching, step bunching is always more pronounced on surfaces with higher miscut angles.

B. KMC simulations

Three groups have used kinetic Monte Carlo simulations to study step-flow growth on vicinal SiC{0001} surfaces. Heuell used a one-dimensional model that did not distinguish carbon atoms from silicon atoms.[15] Two inequivalent types of steps were considered and the probabilities for a diffusing adatom to attach to each step from the terraces below and above were treated as independent parameters. A parameter set was found where an initial train of height-one steps bunched into a train of height-six steps. However, trains of $\frac{1}{2}$ unit-cell height steps are commonly observed in experiments, which suggest that a train of single bilayer steps bunches first into a train of $\frac{1}{2}$ unit-cell height steps, which then bunch into full unit-cell height steps.[9,20] Heuell's model does not produce this behavior.

Stout developed a very elaborate KMC simulation that took account of the SiC crystal structure, the transport, adsorption, and surface diffusion of physisorbed precursors, the dissociative chemisorption, surface diffusion, and desorption of dissociated species, and the attachment or detachment of

adatoms to or from step edges.[13] The energy barrier for a particular atom to make an activated Monte Carlo move was taken to be proportional to the product of the coordination numbers of the initial-state site and the final-state site. For growth onto surfaces vicinal to 6*H*-SiC{000$\bar{1}$}, Stout's simulations bunched an initial train of single bilayer steps into a train where two nearby single bilayer steps accompany a four bilayer height step. No bunching into three bilayer height steps or six bilayer height steps was observed.

Finally, Camarda and co-workers used a full lattice KMC model including defect sites to study step-flow growth onto surfaces vicinal to 4*H* SiC(0001).[25] These authors did not treat silicon and carbon atoms as diffusing species; the smallest growth unit considered was a Si-C dimer. Bunching was observed, but the step heights were not reported.

III. SIMULATION MODEL

We have developed a three-dimensional KMC simulation model based on the crystal structure of SiC. In this paper, the model is used to study step-flow etching and step-flow growth of surfaces vicinal to 6*H*-SiC{0001}. Later work will address island nucleation and multilayer roughness on singular surfaces and thermal decomposition of stepped and flat surfaces to produce epitaxial graphene. The starting vicinal surface studied was usually a uniform train of 36 single bilayer steps with a miscut angle of $\sim 15°(25°)$ for miscut oriented toward $\langle 11\bar{2}0\rangle(\langle 1\bar{1}00\rangle)$. Otherwise (see Fig. 2), miscuts oriented toward $[1\bar{1}00]$ were treated using "helicoidal" boundary conditions (HBC) (Ref. 26) along the $[10\bar{1}0]$ direction and periodic boundary conditions (PBC) along the $[11\bar{2}0]$ direction. The typical system size was $216L_1 \times 40L_2$. Miscuts oriented toward $[\bar{1}2\bar{1}0]$ were treated using HBC along the $[11\bar{2}0]$ direction and PBC along the $[10\bar{1}0]$ direction. The typical system size was $72L_1 \times 216L_2$.

The standard KMC method[27] identifies a set of elementary "moves" and catalogs their relative rates. For our simulations, thermal desorption directly into the gas phase was not allowed, but all atoms (except fully coordinated bulk atoms) were permitted to move to empty nearest-neighbor or next-nearest-neighbor surface sites (with equal probability) at a rate $R=R_0 \exp(-E/k_BT)$, where $R_0=10^{13}$/s, k_B is Boltzmann's constant, and T is the substrate temperature ($T \simeq 1000$ K for most of our simulations). The activation energy E depends on the atom type and its local coordination through a bond-counting rule that includes only the four possible nearest neighbors. All the simulations we report used

$$E_{\mathrm{Si}} = \sum_{1\mathrm{st\ coord.sphere}} E_{\mathrm{Si\text{-}C}} + \sum_{1\mathrm{st\ coord.sphere}} E_{\mathrm{Si\text{-}Si}},$$

$$E_{\mathrm{C}} = \sum_{1\mathrm{st\ coord.sphere}} E_{\mathrm{Si\text{-}C}} + \sum_{1\mathrm{st\ coord.sphere}} E_{\mathrm{C\text{-}C}}, \qquad (1)$$

with $E_{\mathrm{Si\text{-}C}}=0.75$ eV, $E_{\mathrm{Si\text{-}Si}}=0.35$ eV, and $E_{\mathrm{C\text{-}C}}=0.65$ eV. The absolute values of these parameters are not crucial because they only represent *effective* pair-bond energies. What matters is their relative ordering, which reflects (i) the stability of the SiC crystal and (ii) the much greater strength of the C-C bond compared to the Si-Si bond.

We come now to the crucial feature that distinguishes our simulations from others. For one species type (C or Si), the surface jump rate computed using Eq. (1) is exactly the same when the atom sits on any of the six 6*H* (0001)-type terraces (called A, B, C, A^*, C^*, and B^* in Fig. 1) exposed by a vicinal surface with only single bilayer steps. However, the beyond-nearest-neighbor interactions that energetically distinguish the many different polytypes of SiC from one other imply that the energy barriers to surface migration cannot be exactly the same for all six terraces. The relevant surface-diffusion barriers have not been reliably computed or measured. However, the first-principles surface total-energy calculations of Righi *et al.*[28] show a clear energetic preference for SiC(0001) surfaces to continue their subsurface stacking order. This conclusion agrees with the observation that 3C polytype islands nucleate on 4*H*-SiC(0001) and 6*H*-SiC(0001) substrates and with observed stable surface terminations for these exposed faces.[18,29,30] Accordingly, we use the surface-energy ordering computed in Ref. 28 to scale the energy barriers for terrace surface diffusion. The scaling factors used were 1.0 for the atoms sitting on A and A^* terraces, 1.15 for the atoms sitting on C and B^* terraces, and 1.3 for the atoms sitting on B and C^* terraces. This procedure is consistent with our use of the binding energies in Eq. (1) to estimate the bare energy barrier. Our choice of the scaling factors, or more exactly their ordering, is in agreement with the relative stability of the inequivalent terraces implied by the three different step velocities observed during the step-flow growth of graphene by the decomposition of vicinal 6*H*-SiC(0001).[31]

Etching was simulated very simply. Every time an atom was selected to move along the surface, it was instead removed entirely from the simulation with a probability ϵ, where $0<\varepsilon\leq 1$. The etching results were quite insensitive to the exact value of ϵ. To study growth, we ignored precursor effects and deposited silicon and carbon with equal probability at randomly chosen empty surface sites of the SiC lattice. The average deposition rate used, $F=100$/s, corresponds to a typical SiC growth rate of ~ 1 μm/h.

IV. RESULTS

Our model produces very similar results for growth and etching of the Si-terminated face and C-terminated face of 6*H* SiC. This differs from the experimental observations summarized in Sec. II. For that reason, this section reports results only for the Si-terminated face. The C-terminated face is discussed in Sec. V D.

A. Si face with vicinal miscut toward $\langle 1\bar{1}00\rangle$

Figure 3 shows a sequence of simulated morphologies during step-flow *growth* onto a vicinal 6*H*-SiC(0001) surface with the miscut toward the $[1\bar{1}00]$ direction. The step bunches that eventually form have the height of one 6*H* unit cell (six bilayers). Note, however, that $\frac{1}{2}$ unit-cell height steps (three bilayers) form first. The faster growing bunch

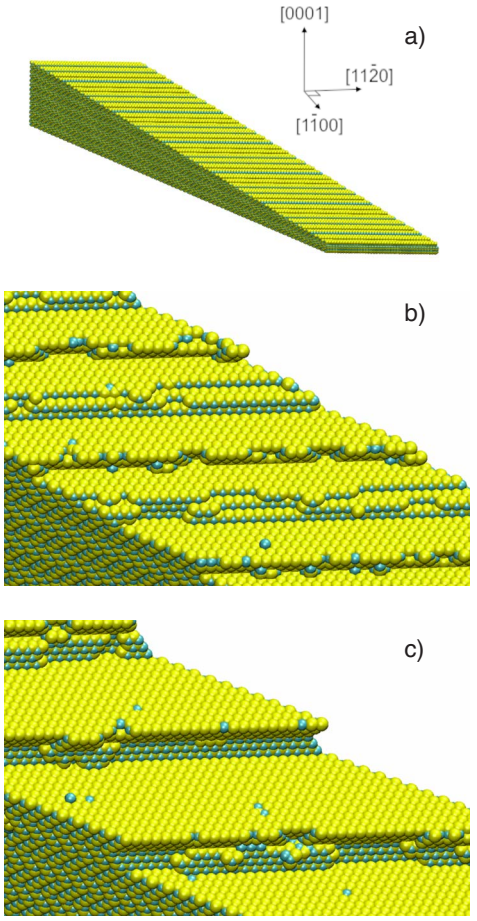

FIG. 3. (Color online) Growth-induced step bunching on vicinal 6*H*-SiC(0001) surface with miscut toward [1$\bar{1}$00].

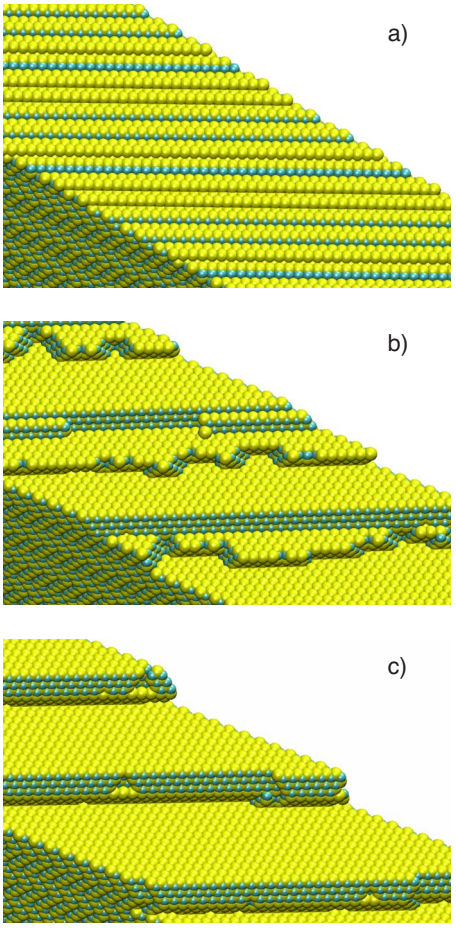

FIG. 4. (Color online) Etching-induced step bunching on vicinal 6*H*-SiC(0001) surface with miscut toward [1$\bar{1}$00].

($A^*C^*B^*$) catches up with the slower growing bunch (*ABC*) to form the final full unit-cell height bunch. The step edges of the final bunches are mostly straight and aligned along the [11$\bar{2}$0] direction, which is the energetically most stable configuration. The overhanging step risers produced by the simulation is an artifact of the nearest-neighbor approximation used in Eq. (1). A less steep (and smoother) step occurs when next nearest neighbors are included but at the cost of a much slower simulation. This change introduces no qualitative effects on the bunching, so we used only the simpler model in this paper.

For comparison with Fig. 3, Fig. 4 shows a sequence of simulated morphologies during the step-flow *etching* of a vicinal 6*H*-SiC(0001) surface with the miscut toward the [1$\bar{1}$00] direction. The etching morphology we obtain is similar to the growth morphology except that the ($A^*C^*B^*$) bunch retracts faster than (*ABC*), and ends up at the bottom of the full unit-cell height step. During growth, the ($A^*C^*B^*$) bunch winds up on top of the (*ABC*) bunch. It is interesting to note that many experiments precede epitaxial growth of 6*H*-SiC with a gas etching step to smoothen the surface. To study this case, we performed a growth simulation beginning with the surface shown in the last panel of Fig. 4. As shown in Fig. 5, the starting full unit-cell height step with (*ABC*) on top of ($A^*C^*B^*$) flips during the growth to a full unit-cell height step with ($A^*C^*B^*$) on top of (*ABC*). In other words, the starting surface does not matter and the final panel of Fig. 3 is the same as the final panel of Fig. 5.

B. Si face with vicinal miscut toward ⟨11$\bar{2}$0⟩

Figure 6 shows a sequence of simulated morphologies during step-flow growth onto a vicinal 6*H*-SiC(0001) surface with the miscut toward the [$\bar{1}$2$\bar{1}$0] direction. We observe the formation of $\frac{1}{2}$ unit-cell height steps with zigzag shaped step edges. On average, the steps are aligned along the [10$\bar{1}$0] direction (perpendicular to the miscut direction). However, the straight segments of the step edges are aligned along the close-packed ⟨11$\bar{2}$0⟩ directions. Etching produces very similar results in the sense that $\frac{1}{2}$ unit-cell height steps form. This is shown in Fig. 7.

V. DISCUSSION

The results of our KMC simulations are in good qualitative agreement with experiments. The formation of full unit-cell height steps (six bilayers) is inherent in SiC step-flow growth or etching on vicinal 6*H*-SiC(0001) surfaces with the miscut toward ⟨1$\bar{1}$00⟩. On the other hand, $\frac{1}{2}$ unit-cell height

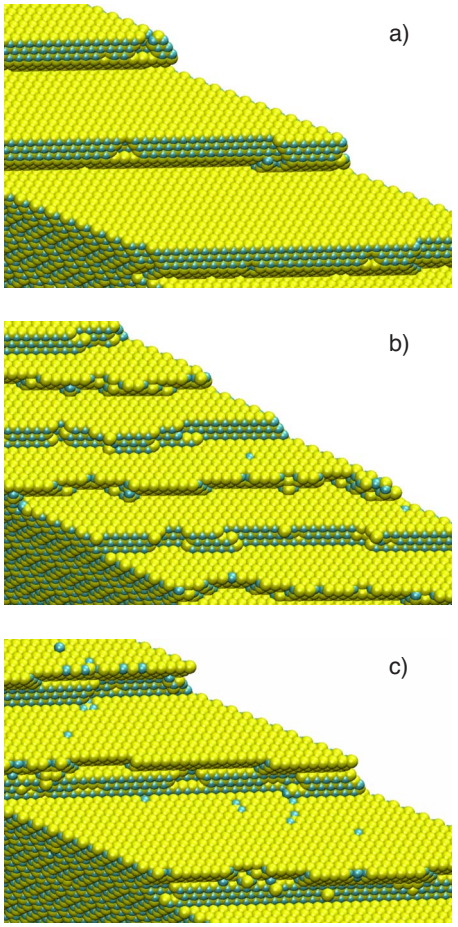

FIG. 5. (Color online) Growth-induced step bunching on vicinal 6*H*-SiC(0001) surface with miscut toward $[1\bar{1}00]$. Initial surface configuration corresponds to etching-induced train of one unit-cell height steps.

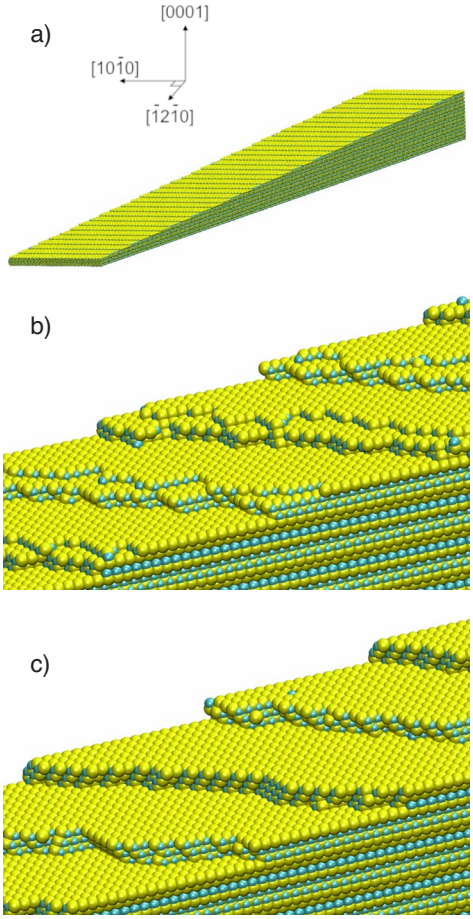

FIG. 6. (Color online) Growth-induced step bunching on vicinal 6*H*-SiC(0001) surface with miscut toward $[11\bar{2}0]$.

steps form during simulations of growth or etching when the miscut is along $\langle 11\bar{2}0\rangle$. We understand all these features in terms of the six different steps that appear on any surface composed of only bilayer height steps (top panel of Fig. 4 or Fig. 7). There are six different velocities because there are three inequivalent terraces where surface diffusion events occur and two inequivalent step edges, where attachment, detachment, and interlayer transport events occur. As described in Sec. III, the surface diffusion rate is fastest for adatoms sitting on A and A^* terraces, slower for adatoms sitting on C and B^* terraces, and slowest for adatoms sitting on B and C^* terraces. Figure 8 shows the two types of steps.[32,33] For the S_N step, a next-to-next nearest-neighbor jump is required for an atom to attach to the step from its upper bounding terrace. Moreover, after this jump occurs, the attached atom is only singly bonded to the step and thus easily detached. For the S_D step, only a next-nearest-neighbor jump is required for an atom to attach to the step from its upper bounding terrace. After this jump occurs, the attached atom is doubly bonded to the step and thus less likely to detach.

Figures 9 and 11 show scenarios for growth and etching, respectively. The fastest steps during growth are bounded from above by the most stable terraces (A and A^*). The slowest steps during growth are bounded from above by the least stable terraces (C and B^*). For the same reason of stability, fast growing steps are the slowest etching and vice versa. Accordingly, the terraces exposed at the time when $\frac{1}{2}$ unit-cell height steps are present on the surface, in both cases correspond to A and A^* (see Fig. 1), which is in agreement with experiments.[21]

A. Step-flow growth

The top panel of Fig. 9 shows a vicinal surface composed of single bilayer steps. The arrows on the steps reflect their relative velocities due to the rates of surface diffusion on the three inequivalent terraces mentioned just above. As a result, the single bilayer steps bunch into the $\frac{1}{2}$ unit-cell height steps shown in the second panel of Fig. 9. The subsequent bunching of these steps into the full unit-cell height step shown in the final panel of Fig. 9 occurs because one half-cell height step is S_N type and the other is S_D type. The latter moves faster than the former because the next-to-next nearest-neighbor jump required for attachment to the S_N step from above is not allowed in our model. In reality, we presume there is simply a higher barrier for this process to occur at a S_N step than at a S_D step. In other words, the Ehrlich-Schwoebel barriers associated with these steps are different.[34,35]

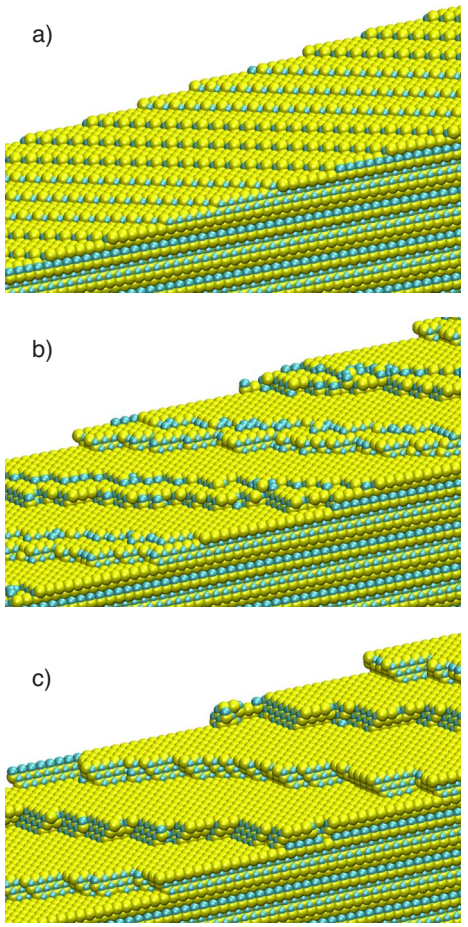

FIG. 7. (Color online) Etching-induced step bunching on vicinal 6*H*-SiC(0001) surface with miscut toward $[11\bar{2}0]$.

The preceding discussion applies directly for vicinal miscuts toward the $\langle 1\bar{1}00\rangle$ direction. However, we have stated that full unit-cell height steps do not form in our SiC growth simulations for miscuts toward the $\langle 11\bar{2}0\rangle$ direction. This occurs because the step edges in this case have a natural zigzag shape, consisting of alternating straight segments, corresponding to S_N or S_D steps (see Fig. 10). Each step edge has equal portions of S_N and S_D steps, and as a result, all $\frac{1}{2}$ unit-cell height steps propagate with the same speed. Of course, if the miscut is not exactly toward the $\langle 11\bar{2}0\rangle$ direction, adjacent $\frac{1}{2}$ unit-cell height steps differ in their relative population of S_N and S_D step edges. This may trigger the formation of full unit-cell height steps.

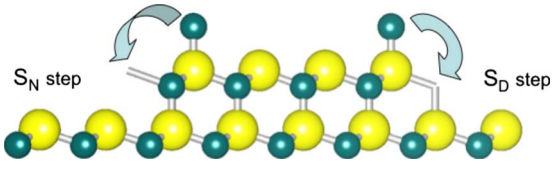

FIG. 8. (Color online) Side view of S_N and S_D steps. See text for discussion.

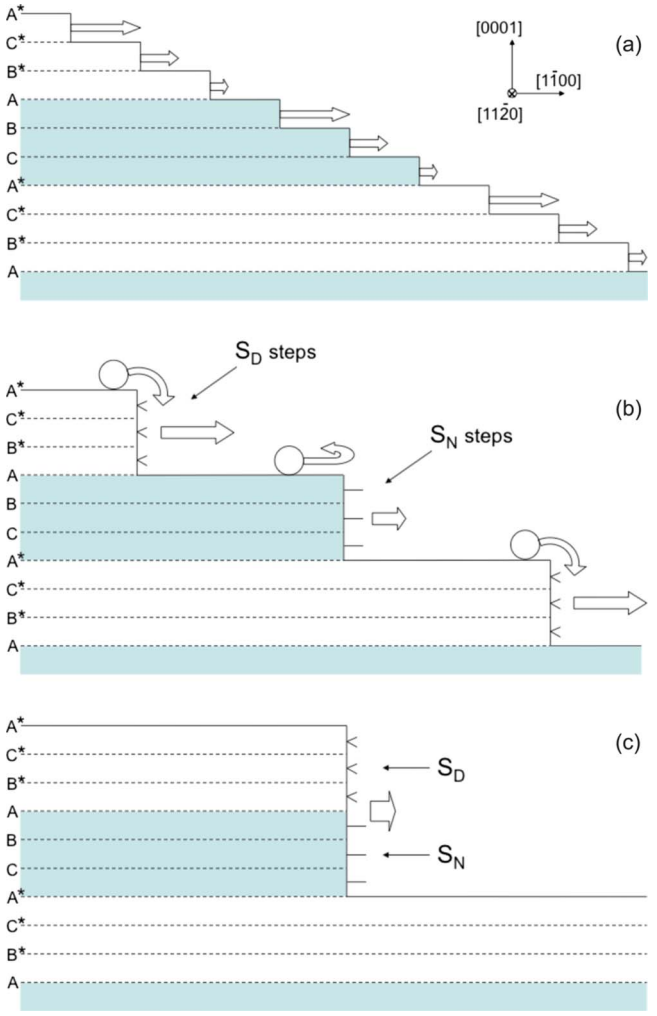

FIG. 9. (Color online) A cartoon of step-flow growth on 6*H* SiC(0001): (a) different length arrows indicate the different growth velocities of the steps which terminate the three inequivalent bilayer terraces; (b) two types of $\frac{1}{2}$ unit-cell height steps (S_N and S_D) differ by the number of dangling bonds for the outermost step edge atoms. The presence of an Ehrlich-Schwoebel energy barrier to downward interlayer diffusion at S_N steps explains the difference in growth speed between S_N and S_D $\frac{1}{2}$ unit-cell height step bunches; (c) S_D steps wind up on top of S_N steps to form a single, full unit-cell height step.

B. Step-flow etching

Etching is often regarded as the inverse of growth.[16,20] Therefore, mimicking our discussion of growth, the top panel of Fig. 11 shows a vicinal surface composed of single bilayer steps. The arrows on the steps reflect their etch velocities due to the different step detachment rates associated with the three inequivalent terraces discussed earlier. As a result, the steps bunch to form the $\frac{1}{2}$ unit-cell height steps shown in the second panel of Fig. 11. The subsequent bunching of these steps into the full unit-cell height step shown in the final panel of Fig. 9 occurs because the S_N-type step, which has triply bonded outermost atoms, etches more slowly than the S_D-type step which has only doubly bonded outermost atoms.

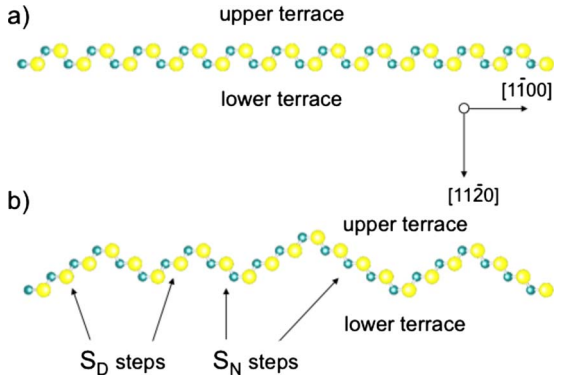

FIG. 10. (Color online) (a) A step edge of the so-called "open" step (top view), aligned along $\langle 1\bar{1}00\rangle$, is shown schematically. (b) Growth and etching at such steps typically result in development of triangular protrusions. The alternating straight segments of this protrusions (S_N and S_D step edges) are aligned along the $\langle 11\bar{2}0\rangle$ directions.

In agreement with experiments, we observe the development of "triangular" protrusions (see Fig. 4) which form as a result of etching at S_D step bunches.[33] As Fig. 12 shows, the straight segments of these protrusions are aligned at angles of 30° with respect to the direction of miscut ($[1\bar{1}00]$) and thus correspond to energetically stable S_N step bunches. As discussed in detail in Ref. 33, the outermost atoms of these protrusions, which have only two bonds with nearest neighbors, constitute another source of instability. As a result, preferential etching of these protrusions leads to the formation of full unit-cell height steps.

In our simulations of SiC etching for miscut toward $\langle 11\bar{2}0\rangle$, we do not observe the formation of unit-cell height steps. This agrees with the most recent experimental results.[19–21] We explain this in terms of the previously discussed zigzag structure of the steps which occur on this surface. Each $\frac{1}{2}$ unit-cell height step with a zigzag shape has equal portions of faster and slower etched straight segments, which correspond to S_D and S_N step bunches. For this reason the etching rates of all $\frac{1}{2}$ unit-cell height steps are identical (on average) and unit-cell height steps do not form.

Notwithstanding the foregoing, some etching experiments on surfaces with miscut toward $\langle 11\bar{2}0\rangle$ *do* see the formation of full unit-cell height steps.[16,18,21] A possible explanation for these conflicting observations is the previously mentioned possibility of deviations of the miscut from exactly $\langle 11\bar{2}0\rangle$ with its attendant steps with faster and slower etching segments. When the populations of these segments are not equal, the $\frac{1}{2}$ unit-cell height steps with more fast-etching segments catch up to the steps with fewer fast-etching segments.[19,21] The result is a train of full unit-cell height steps.

C. Surface terminations

Only one type of terrace is exposed to the vacuum after all full unit-cell steps have formed on a $[1\bar{1}00]$ miscut surface. However, our KMC simulations predict that the exposed terrace is not the same after growth as it is after etching. After growth, the $A^*C^*B^*$ bunch (the outermost atoms of bilayer steps have two bonds with nearest neighbors and two dangling bonds) is on top of the ABC bunch (the outermost atoms of bilayer steps have three bonds with nearest neighbors and one dangling bond). This is called the S_3^* surface termination in the literature.[21] After etching, the sequence of bilayers at the surface is opposite: $\ldots B^*C^*A^*CBA$. This is called the S_3 surface termination. Cross-section TEM experiments could be used to test this prediction.

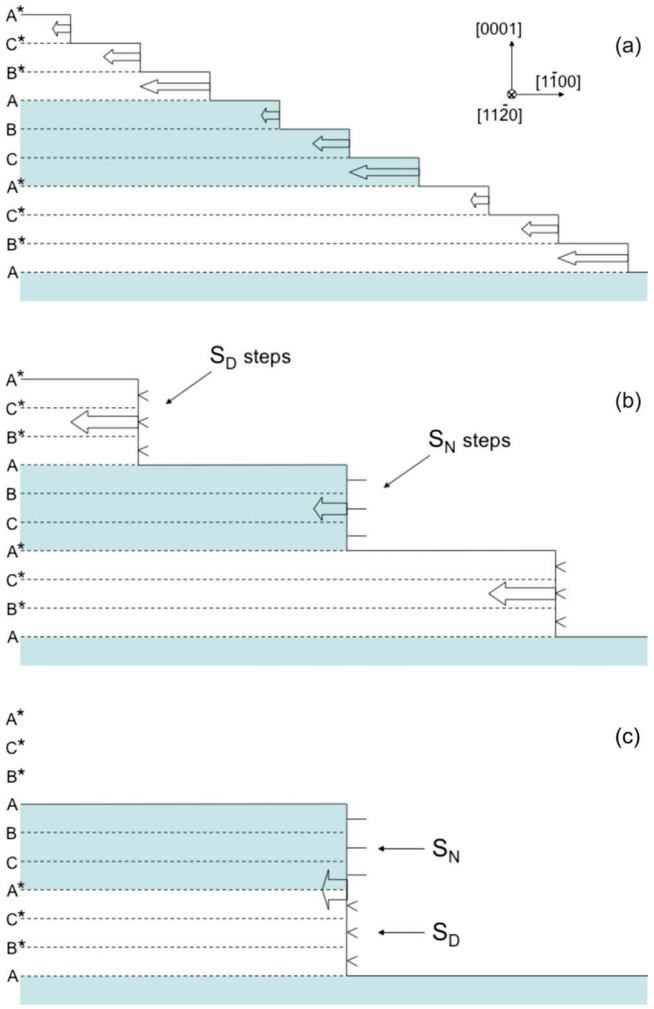

FIG. 11. (Color online) A cartoon of step-flow etching of 6*H* SiC(0001): (a) different length arrows indicate the different etch velocities of the steps which terminate the three inequivalent bilayer terraces; (b) two types of $\frac{1}{2}$ unit-cell height steps (S_N and S_D) have different edge velocities because they differ in the number of dangling bonds for the outermost step edge atoms; (c) S_N steps wind up on top of S_D steps to form a single, full unit-cell height step.

D. C-terminated surface

The simulation results we have presented so far describe the evolution of surface morphology during the epitaxial growth or etching of 6*H*-SiC on the vicinal 6*H*-SiC(0001) surface (Si-terminated face). Our simulation results for the C-terminated face [6*H*-SiC(000$\bar{1}$)], using the same model

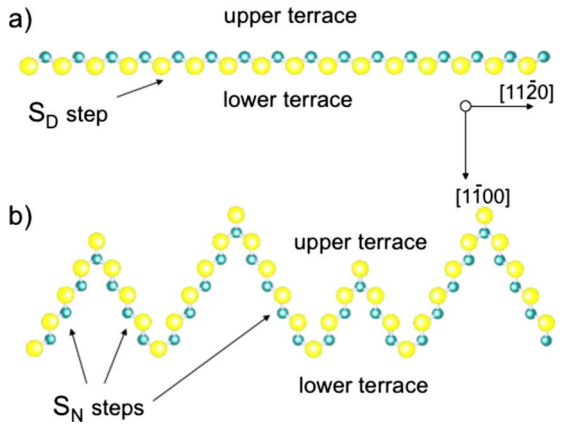

FIG. 12. (Color online) (a) S_D step edge (top view) is shown schematically. (b) S_D steps are less stable then S_N steps because the outermost atoms of the former have two nearest-neighbor bonds, while the outermost atoms of the latter have three such bonds. Growth and etching are faster at S_D steps and typically result in development of triangular protrusions. The straight segments of this protrusions are aligned along the $\langle 11\bar{2}0\rangle$ directions and correspond to energetically stable S_N steps.

parameters, are qualitatively very similar. This disagrees with the step-bunching behavior observed in experiments which is typically less pronounced for the C face compared to the Si face.[9,20] On the other hand, the C-face data are quite explicable if the terrace diffusion rates and step mobilities differ from their values on the Si face.

The terrace diffusion scaling factors used to take account of the three inequivalent terraces of SiC(0001) were chosen based on the Si-face calculations of Righi *et al.*[28] These authors did not perform similar calculations for the C face and it is possible that the results are different. One possibility is that the scale factor ordering is the same as for the Si face but that their magnitudes are less different. Another possibility is that the ordering of the scale factors differs on the C face. Experimental support for this comes from the different surface terminations observed for the two polar faces of 6*H*-SiC{0001}. The so-called $(2\times 2)_C$ reconstruction, which stabilizes hexagonal stacking at the surface (S_1-stable surface termination) is sometimes observed on the C face.[36] This implies a different ordering for the three inequivalent terrace scaling factors than for the Si face.

It seems quite likely that the Ehrlich-Schwoebel barriers to interlayer diffusion (which strongly influence the bunching of half unit-cell height steps into full unit-cell height steps in our model) are different on the C face and the Si face. The magnitude of these barriers is intimately connected to the structure of the steps and there is theoretical evidence that the step structure indeed depends on the polarity of the surface.[37] If the difference between the corresponding barriers is less pronounced for the C face, we would find the experimentally observed delay in the formation of full unit-cell height steps during the growth of 6*H*-SiC on the vicinal 6*H*-SiC$(000\bar{1})$ surface. Moreover, strong barriers to interlayer diffusion at both S_N and S_D steps suppress interlayer mass transport and stabilize the persistence of single bilayer steps. This would explain the observed experimentally preference of bilayer height steps on C-terminated surfaces to remain completely unbunched during growth.[9]

Finally, it is possible that step bunching is less pronounced on the C face because the elastic-driven repulsive interaction between the steps of a vicinal surface[38] is more pronounced on the C face compared to the Si face. The repulsion depends on the step stiffness,[39] which in turn depends on the step structure, which is doubtless different for the two faces.

VI. CONCLUSIONS

We have used lattice KMC simulations to study the formation of step bunches during growth and etching of 6*H*-SiC(0001) vicinal surfaces. For both situations, the simulations show that single bilayer steps bunch into half unit-cell steps (three bilayers each) which subsequently bunch into full unit-cell steps. This is consistent with experimental observations for both the Si-terminated face and the C-terminated face except that we obtain greater bunching for the C face than seen in experiment. The main driving force for bunching into half unit-cell height steps is that surface diffusion is not equally fast on all bilayer terraces. The main driving force for the subsequent bunching into full height unit cells is the existence of two different local atomic step structures which leads to two different step mobilities. A prediction of the model which invites an experimental test is that growth-induced and etching-induced step bunching lead to different surface terminations for the exposed terraces when full unit-cell steps are present.

ACKNOWLEDGMENTS

The authors acknowledge helpful correspondence with Randall Feenstra and Miron Hupalo. The work of V.B. was supported by the Department of Energy under Grant No. DE-FG02-04-ER46170. We also acknowledge a grant of computer time from the National Center for Supercomputing Applications.

*valery.borovikov@physics.gatech.edu
†andrew.zangwill@physics.gatech.edu

[1] H. Matsunami and T. Kimoto, Mater. Sci. Eng. R. **20**, 125 (1997).
[2] A. Fissel, Phys. Rep. **379**, 149 (2003).
[3] R. F. Davis, S. Tanaka, and R. S. Kern, J. Cryst. Growth **163**, 93 (1996).
[4] H. Okumura, M. Horita, T. Kimoto, and J. Suda, Appl. Surf. Sci. **254**, 7858 (2008).
[5] J. Hass, W. A. de Heer, and E. H. Conrad, J. Phys.: Condens.

Matter **20**, 323202 (2008).
[6] J. A. Powell and D. J. Larkin, Phys. Status Solidi B **202**, 529 (1997).
[7] N. Ohtani, M. Katsuno, J. Takahashi, H. Yashiro, and M. Kanaya, Phys. Rev. B **59**, 4592 (1999).
[8] V. Papaioannou, J. Stoemenos, L. Di Cioccio, D. David, and C. Pudda, J. Cryst. Growth **194**, 342 (1998).
[9] T. Kimoto, A. Itoh, H. Matsunami, and T. Okano, J. Appl. Phys. **81**, 3494 (1997).
[10] S. Tanaka, R. S. Kern, R. F. Davis, J. F. Wendelken, and J. Xu, Surf. Sci. **350**, 247 (1996).
[11] V. Heine, C. Cheng, and R. J. Needs, J. Am. Ceram. Soc. **74**, 2630 (1991).
[12] F. R. Chien, S. R. Nutt, W. S. Yoo, T. Kimoto, and H. Matsunami, J. Mater. Res. **9**, 940 (1994).
[13] P. J. Stout, J. Vac. Sci. Technol. A **16**, 3314 (1998).
[14] T. Frisch and A. Verga, Phys. Rev. Lett. **94**, 226102 (2005).
[15] P. Heuell, M. A. Kulakov, and B. Bullemer, Inst. Phys. Conf. Ser. **137**, 353 (1994); Surf. Sci. **331-333**, 965 (1995).
[16] S. Nakamura, T. Kimoto, H. Matsunami, S. Tanaka, N. Teraguchi, and A. Suzuki, Appl. Phys. Lett. **76**, 3412 (2000).
[17] S. Nakamura, T. Kimoto, and H. Matsunami, J. Cryst. Growth **256**, 341 (2003); S. Nakamura, *ibid.* **256**, 347 (2003).
[18] H. Nakagawa, S. Tanaka, and I. Suemune, Phys. Rev. Lett. **91**, 226107 (2003).
[19] A. Nakajima, H. Yokoya, F. Furukawa, and H. Yonezu, J. Appl. Phys. **97**, 104919 (2005).
[20] S. Nie, C. D. Lee, R. M. Feenstra, Y. Ke, R. P. Devaty, W. J. Choyke, C. K. Inoki, T. S. Kuan, and G. Gu, Surf. Sci. **602**, 2936 (2008).
[21] K. Hayashi, K. Morita, S. Mizuno, H. Tochihara, and S. Tanaka, Surf. Sci. **603**, 566 (2009).
[22] H. S. Kong, J. T. Glass, and R. F. Davis, J. Appl. Phys. **64**, 2672 (1988).
[23] T. Ueda, H. Nishino, and H. Matsunami, J. Cryst. Growth **104**, 695 (1990).
[24] M. Syväjärvi, R. Yakimova, and E. Janzén, J. Cryst. Growth **236**, 297 (2002).
[25] M. Camarda, A. La Magna, and F. La Via, J. Comput. Phys. **227**, 1075 (2007); M. Camarda, A. La Magna, P. Fiorenza, F. Giannazzo, and F. La Via, J. Cryst. Growth **310**, 971 (2008).
[26] M. Camarda, A. La Magna, and F. La Via, J. Comput. Phys. **227**, 1075 (2007).
[27] A. B. Bortz, M. H. Kalos, and J. L. Lebowitz, J. Comput. Phys. **17**, 10 (1975).
[28] M. C. Righi, C. A. Pignedoli, G. Borghi, R. Di Felice, C. M. Bertoni, and A. Catellani, Phys. Rev. B **66**, 045320 (2002).
[29] U. Starke, J. Schardt, J. Bernhardt, M. Franke, and K. Heinz, Phys. Rev. Lett. **82**, 2107 (1999).
[30] K. Heinz, J. Bernhardt, J. Schardt, and U. Starke, J. Phys.: Condens. Matter **16**, S1705 (2004).
[31] M. Hupalo, E. Conrad, and M. C. Tringides, arXiv:0809.3619 (unpublished).
[32] R. J. Pechman, X.-S. Wang, and J. H. Weaver, Phys. Rev. B **52**, 11412 (1995).
[33] V. Ramachandran, M. F. Brady, A. R. Smith, R. M. Feenstra, and D. W. Greve, J. Electron. Mater. **27**, 308 (1998).
[34] G. Ehrlich and F. G. Hudda, J. Chem. Phys. **44**, 1039 (1966); R. L. Schwoebel, J. Appl. Phys. **40**, 614 (1969).
[35] T. Michely and J. Krug, *Islands, Mounds and Atoms*, Springer Series in Surface Science Vol. 42 (Springer, New York, 2004).
[36] A. Seubert, J. Bernhardt, M. Nerding, U. Starke, and K. Heinz, Surf. Sci. **454-456**, 45 (2000).
[37] E. Pearson, T. Takai, T. Halicioglu, and W. A. Tiller, J. Cryst. Growth **70**, 33 (1984).
[38] P. Müller and A. Saúl, Surf. Sci. Rep. **54**, 157 (2004).
[39] V. I. Marchenko and A. Y. Parshin, Zh. Eksp. Teor. Fiz. **79**, 257 (1980) [Sov. Phys. JETP **52**, 129 (1980)].